Low-Thrust Attitude Control for Nano-Satellite with Micro-Cathode Thrusters

IEPC-2013-366

Presented at the 33rd International Electric Propulsion Conference,
The George Washington University, Washington, D.C., USA
October 6–10, 2013

Tse-Huai Wu*, Taeyoung Lee† and Michael Keidar‡
The Goerge Washington University, Washington, DC, 20052, USA

Micro-cathode arc thruster (μCAT) has been proposed for nano-satellite propulsion. The physical constraints of the μCAT, namely the constraint of low thrust due to small available energy plays an important role in designing the controller. One must ensure the control effect and the closed-loop stability while considering the limitation of the control input. The bounded control input or control input saturation for the spacecraft attitude control has been investigated.

In this paper , a controller is proposed to apply in the μCAT which is integrated to a 6U CubeSat. The design of the controller must take into account the magnitude of the control torque, since the thrust provided by the μCAT is quite small.

I. Introduction

Micro-cathode arc thruster (μCAT) has been designed and developed by the Micro-propulsion and Nanotechnology Laboratory (MpNL) from the George Washington University. The μCAT has tubular titanium electrodes, one cathode and one anode, separated by ceramic substance as the isolator. The erosion of the cathode tube, due to an electrical arc discharge, is in the form of plasma. There is a magnetic coil mounted around the anode which generates a magnetic field to direct and concentrate the plasma that offers propulsion. The properties and performance of the μCAT have been studied.[1,2] With low mass (less than 300g) and low operating voltage (10∼30 VDC), the μCAT is suitable for the small satellite applications such as CubeSats.

Considering the thrust provided by μCAT is quite small, the design of the controller must take into account the magnitude of the control torque explicitly. The problem of spacecraft or rigid body control under bounded torque input has been extensively studied in the past decade. An adaptive tracking control algorithm for spacecraft in the presence of input saturation is presented in Ref. 3. Also, in Ref. 4, a bounded controller was proposed to stabilize a rigid body. The work in Ref. 5 presented attitude stabilization of the inverted 3D pendulum with input saturation. The controllers in the aforementioned literatures have one common feature is that they are partially or fully bounded by the classical saturation function. In addition, hyperbolic tangent function is also introduced to guarantee the boundedness of the control input since it is continuously differentiable.[6,7,8] In this paper, inspired and modified from the classic saturation function, a different function is presented to bound the control input.

One of the distinct features of this paper is that we construct the control system directly on the special orthogonal group, $\mathsf{SO(3)}$, which is the configuration manifold of attitude. As a result, the proposed control system can represent an attitude without singularity and ambiguity by following the geometric control approach.[9] Except Ref. 5, most of the literatures use attitude parameterizations such as quaternions (Euler parameters) or the modified Rodrigues parameters (MRP) which are unable to represent attitude uniquely and globally. The MRP is geometrically singular since it is not defined for 180° of rotation.[10] Without

*PhD. student, Department of Mechanical and Aerospace Engineering, wu52@gwu.edu
†Assistant Professor, Department of Mechanical and Aerospace Engineering, tylee@gwu.edu
‡Associate Professor, Department of Mechanical and Aerospace Engineering, keidar@gwu.edu

singularities, quaternions double cover $\mathsf{SO(3)}$ in the presence of ambiguity, that is, two different quaternions correspond to the same attitude. Hence, a quaternion-based controller may exhibit the well-known unwinding behavior which is an undesirable phenomena since it cause unnecessarily large-angle rotations.[11]

II. Problem Statement

A. Spacecraft Attitude Dynamics

The equations of motion for the attitude dynamics of CubeSat are given by

$$J\dot{\Omega} + \Omega \times J\Omega = u, \tag{1}$$

$$\dot{R} = R\hat{\Omega}, \tag{2}$$

where $R \in \mathsf{SO(3)}$ is a rotation matrix representing the attitude of CubeSat, $J \in \Re^{3\times 3}$ is the inertia matrix. Also, $\Omega \in \Re^3$ and $u \in \Re^3$ are angular velocity control moment generated by micro-cathode thrusters, respectively. J, Ω and u are all represented with respect to the body-fixed frame. The *hat* map $\wedge : \Re^3 \to \mathfrak{so}(3)$ transforms a vector in $\Re^3$ to a 3×3 skew-symmetric matrix such that $\hat{x}y = (x)^\wedge y = x \times y$ for any $x, y \in \Re^3$. The inverse of the hat map is denoted by the *vee* map $\vee : \mathfrak{so}(3) \to \Re^3$. Few properties of the hat map are listed as follows:

$$\hat{x}y = x \times y = -y \times x = -\hat{y}x, \tag{3}$$

$$\hat{x}A + A^\mathsf{T}\hat{x} = (\{\mathrm{tr}[A]I_{3\times 3} - A\}x)^\wedge, \tag{4}$$

$$R\hat{x}R^\mathsf{T} = (Rx)^\wedge, \tag{5}$$

for any $x, y, z \in \Re^3$, $A \in \Re^{3\times 3}$, and $R \in \mathsf{SO(3)}$. Throughout this paper, the 2-norm of a matrix A is denoted by $\|A\|$ and $I_{3\times 3}$ denotes the 3 by 3 identity matrix. In addition, the dot product of two vectors can be denoted in the form of matrix transpose, namely, $x \cdot y = x^\mathsf{T} y$.

Assuming that the mass is uniformly distributed over CubeSat, its inertia matrix is given by

$$\begin{aligned} J &= \frac{1}{12} 6\,\mathrm{kg} \times \mathrm{diag}[(0.3^3 + 0.1^2),\ (0.2^3 + 0.1^2),\ (0.2^3 + 0.3^2)]\mathrm{m}^2 \\ &= \mathrm{diag}[5,\ 2.5,\ 6.5] \times 10^{-2}\,\mathrm{kgm}^2. \end{aligned}$$

B. Thruster Model

The total mass of the 6U CubeSat is $m = 6\,\mathrm{kg}$ with the volume $0.3\,\mathrm{m} \times 0.2\,\mathrm{m} \times 0.1\,\mathrm{m}$. One micro-cathode thruster generates a thrust of $10\,\mu\mathrm{N}$ per watt. It is assumed that 0.5 watt is available for one thruster. In addition, assuming that there are 5 micro-cathode thrusters with the average distance to center of mass $0.1\,\mathrm{m}$, the maximum torque is given by

$$\tau_{\max} = 0.1\,\mathrm{m} \times (10 \times 10^{-6}\,\mathrm{N/Watt} \times 0.5\mathrm{Watt}) \times 5 = 2.5 \times 10^{-6}\,\mathrm{Nm}. \tag{6}$$

C. Saturation Function

The classic normalized saturation function is one of the most common way to bound the control input:

$$\mathrm{sat}(x) = \begin{cases} 1, & \text{for} \quad x > 1 \\ x, & \text{for} \quad -1 \le x \le 1 \\ -1, & \text{for} \quad x < -1 \end{cases}$$

where $x \in \Re$ is a scalar. Consider the classic saturation function is applied to two linearly independent vectors, X_1, $X_2 \in \Re^3$. If all the elements of X_1, X_2 are greater than 1, then $\mathrm{sat}(X_1) = \mathrm{sat}(X_2) = [1, 1, 1]$. As a result, the classical saturation function not only restricts the range of X_1 and X_2, it may also eliminates the direction difference between them. In this paper, instead of using $\mathrm{sat}(\cdot)$, a different saturation function is introduced:

$$\mathfrak{sat}(X) \triangleq \begin{cases} \frac{1}{\|X\|} X, & \text{for} \quad \|X\| > 1 \\ X, & \text{for} \quad \|X\| \le 1 \end{cases} \tag{7}$$

where $X \in \Re^3$. Notice that $\|\mathfrak{sat}(X)\| \leq 1$. The new saturation function $\mathfrak{sat}(\cdot)$ puts a limit on the magnitude of a vector while preserving the directional property.

III. Geometric Control on $\mathsf{SO(3)}$

The kinematic equation for the given smooth attitude command $R_d \in \mathsf{SO(3)}$ is given as

$$\dot{R}_d = R_d \hat{\Omega}_d, \tag{8}$$

where $\Omega_d \in \Re^3$ is the desired angular velocity.

A. Attitude Error Dynamics

First, to describe the attitude error, we define

$$Q = R^{\mathsf{T}} R_d, \tag{9}$$

where Q is the relative attitude of the desired attitude with respect to the current attitude. It can be shown that $R = R_d$ if and only if $Q = I$.

The attitude error dynamics of a rigid body has been studied and presented in Ref. 9. Here we rewrite the Proposition 1, Proposition 2 and the corresponding properties of Ref. 9 as follows.

Proposition 1. The attitude error function $\Psi \in \Re$, the attitude error vector $e_R \in \Re^3$ and the angular velocity vector $e_\Omega \in \Re^3$ are rewritten as follows

$$\Psi = \frac{1}{2}\mathrm{tr}[G(I - Q^{\mathsf{T}})] = \frac{1}{2}\mathrm{tr}[G(I - Q)], \tag{10}$$

$$e_R = \frac{1}{2}(GQ^{\mathsf{T}} - QG)^{\vee}, \tag{11}$$

$$e_\Omega = \Omega - Q\Omega_d, \tag{12}$$

where $G \triangleq \mathrm{diag}[g_1, g_2, g_3] \in \Re^{3\times 3}$ for distinct, positive constants g_1, g_2, and $g_3 \in \Re$. Then, the following statements hold:

(i). Ψ is positive definite about $R = R_d$.

(ii). The left-trivialized derivative of Ψ is given by

$$\mathsf{T}_I^* \mathsf{L}_R (D_R \Psi) = e_R. \tag{13}$$

(iii). The critical point of Ψ, where $e_R = 0$ are $\{R_d\} \bigcup \{R_x \exp(\pi \hat{s})\}$, for $s \in \{e_1, e_2, e_3\}$.

(iv). Ψ is locally quadratic, that is,

$$b_1 \|e_R\|^2 \leq \Psi \leq b_2 \|e_R\|^2, \tag{14}$$

where b_1 and b_2 are constants given by $b_1 = \frac{h_1}{h_2 + h_3}$ and $b_2 = \frac{h_1 h_4}{h_5(h_1 - \psi)}$, respectively. For

$$\begin{aligned}
h_1 &= \min\{g_1 + g_2,\, g_2 + g_3,\, g_3 + g_1\},\\
h_2 &= \max\{(g_1 - g_2)^2,\, (g_2 - g_3)^2,\, (g_3 - g_1)^2\},\\
h_3 &= \max\{(g_1 + g_2)^2,\, (g_2 + g_3)^2,\, (g_3 + g_1)^2\},\\
h_4 &= \max\{g_1 + g_2,\, g_2 + g_3,\, g_3 + g_1\},\\
h_5 &= \min\{(g_1 + g_2)^2,\, (g_2 + g_3)^2,\, (g_3 + g_1)^2\}.
\end{aligned}$$

And, ψ is a positive constant that is strictly less than h_1 also satisfying $\Psi < \psi < h_1$.

(v). The magnitude of the attitude error vector is bounded by

$$\|e_R\| \leq \frac{1}{2}\sqrt{12h_2 + 3h_3}. \tag{15}$$

Proof. The proof of (i)-(iv) is available at Ref. 12. Specifically, from the proof of the Propositon 1 in Ref. 12, we have

$$\|e_R\|^2 = \frac{(1-\cos\|x\|)^2}{4\|x\|^4}\sum_{(i,j,k)\in\mathfrak{C}}(g_i-g_j)^2x_i^2x_j^2 + \frac{\sin^2\|x\|}{4\|x\|^2}\sum_{(i,j,k)\in\mathfrak{C}}(g_i+g_j)^2x_k^2,$$

where $\mathfrak{C} = \{(1,2,3),(2,3,1),(3,1,2)\}$. Considering the fact that $(1-\cos\|x\|)^2 \leq 4$, $\frac{x_i^2x_j^2}{\|x\|^4} \leq 1$, $\sin^2\|x\| \leq 1$ and $\frac{x_k^2}{\|x\|^2} \leq 1$, we can write

$$\|e_R\|^2 \leq 3h_2 + \frac{3}{4}h_3,$$

which shows (v) explicitly. □

Proposition 2. The error dynamics for Ψ, e_R, and e_Ω satisfies the following properties:

$$\dot{Q} = -\hat{e}_\Omega Q, \tag{16}$$

$$\dot{\Psi} = e_R \cdot e_\Omega, \tag{17}$$

$$\dot{e}_R = E(R,R_d)e_\Omega, \tag{18}$$

$$J\dot{e}_\Omega = u + \xi\times e_\Omega - JQ\dot{\Omega}_d - \widehat{Q\Omega_d}(JQ\Omega_d), \tag{19}$$

where the matrix $E(R,R_d) \in \Re^{3\times3}$ and the vector $\xi \in \Re^3$ are given by

$$E(R,R_d) = \frac{1}{2}(\mathrm{tr}[QG]I_{3\times3} - QG), \tag{20}$$

$$\xi = Je_\Omega + (2J - \mathrm{tr}[J]I_{3\times3})Q\Omega_d. \tag{21}$$

In particular, $E(R,R_d)$ and ξ are bounded by

$$\|E(R,R_d)\| \leq \frac{1}{\sqrt{2}}\mathrm{tr}[G], \tag{22}$$

$$\|\xi\| \leq \lambda_M\|e_\Omega\| + B^*, \tag{23}$$

where $B^* \in \Re$ is the upper bound of the term $\|(2J-\mathrm{tr}[J]I_{3\times3})Q\Omega_d\|$, and λ_M is the largest eigenvalue of J.

Proof. All the properties expect Eq. (19) and (21) have been proved in Ref. 12. We start from the substitution of Eq. (12) into (1),

$$J(\dot{e}_\Omega + \dot{Q}\Omega_d + Q\dot{\Omega}_d) + (e_\Omega + Q\Omega_d)\times J(e_\Omega + Q\Omega_d) = u. \tag{24}$$

Applying Eq. (16) to Eq. (24) and rearrangement, we can further obtain

$$J\dot{e}_\Omega = u + J(e_\Omega + Q\Omega_d)\times e_\Omega - (J\widehat{Q\Omega_d} + \widehat{Q\Omega_d}J)e_\Omega - JQ\dot{\Omega}_d - Q\Omega_d\times(JQ\Omega_d). \tag{25}$$

From Eq. (4), one of the map identities, we know that $-(\widehat{Q\Omega_d}J + J\widehat{Q\Omega_d}) = -(\{\mathrm{tr}[J]I_{3\times3} - J\}Q\Omega_d)^\wedge$. Substituting this into Eq. (25) shows Eq. (19) and (21). □

B. Attitude Stabilization with Bounded Control Input

In this section, a control law with bounded magnitude is designed to detumble the CubeSat and reorientate it to specific fixed attitude, that is, $\Omega_d = [0\ 0\ 0]^\mathsf{T}$ and $\dot{R}_d = 0_{3\times3}$.

Proposition 3. Consider the system given by Eq. (1) and (2), for positive constants k_Ω, $k_R \in \Re^+$, we define the following control law:

$$u = -k_\Omega \mathfrak{sat}(\Omega) - k_R e_R. \tag{26}$$

Notice that the angular velocity Ω is bounded by the saturation function $\mathfrak{sat}(\cdot)$ and the magnitude of the attitude error vector e_R is already shown to be restrictd in Eq. (15). In particular, the equilibrium configuration $(R, \Omega) = (R_d, 0)$ is asymptotically stable, with an estimation of region of attraction given by

$$\Psi(R(0), R_d(0)) \leq \psi < h_1, \tag{27}$$

$$\|\Omega(0)\|^2 \leq \frac{2k_R}{\lambda_M}[\psi - \Psi(R(0), R_d(0))]. \tag{28}$$

Proof. The Lyapunov function is specified as

$$\mathcal{V}(R, R_d, e_\Omega) = \frac{1}{2}\Omega^\mathsf{T} J\Omega + k_R\Psi(R, R_d). \tag{29}$$

From (14), we know the Lyapunov function is positive definite.

Using Eq. (1) and (17), the time-derivative of the Lyapunov function becomes

$$\dot{\mathcal{V}}(R, R_d, e_\Omega) = \Omega^\mathsf{T} J\dot{\Omega} + k_R\dot{\Psi}(R, R_d) = \Omega^\mathsf{T}(u - \Omega \times J\Omega) + k_R\Omega^\mathsf{T} e_R. \tag{30}$$

Substituting (26) into this we have

$$\dot{\mathcal{V}}(R, R_d, e_\Omega) = -k_\Omega \mathfrak{sat}(\Omega)^\mathsf{T}\Omega = \begin{cases} -k_\Omega\|\Omega\|, & \text{for} \quad \|\Omega\| > 1 \\ -k_\Omega\|\Omega\|^2, & \text{for} \quad \|\Omega\| \leq 1 \end{cases} \tag{31}$$

which implies the time-derivative of Lyapunov function is negative semi-definite. Note that $\dot{\mathcal{V}} = 0$ implies $\Omega = 0$. Substituting this into (1) we can immediately write

$$0 + 0 \times 0 = -k_\Omega 0 - k_R e_R \Rightarrow e_R = 0. \tag{32}$$

According to the LaSalle's theorem, we now conclude the zero equilibrium is asymptotically stable.

In addition, we can use Eq. (28) to specify the initial condition of $V(t)$,

$$\begin{aligned} V(R(0), R_d(0), e_\Omega(0)) &\leq \frac{1}{2}\lambda_M\|\Omega(0)\|^2 + k_R\Psi(R(0), R_d(0)) \\ &\leq \frac{1}{2}\lambda_M\{\frac{2k_R}{\lambda_M}[\psi - \Psi(R(0), R_d(0))]\} + k_R\Psi(R(0), R_d(0)) = k_R\psi. \end{aligned} \tag{33}$$

Since $V(t)$ is non-increasing, the value of $V(t)$ must be less or equal than $V(0)$, thus we have

$$k_R\Psi(R(t), R_d(t)) \leq V(R(t), R_d(t), e_\Omega(t)) \leq V(R(0), R_d(0), e_\Omega(0)) \leq k_R\psi < k_R h_1, \tag{34}$$

which shows that $\Psi(R(t), R_d(t)) < h_1$ and Eq. (14) is also satisfied. □

C. Attitude Tracking with Bounded Control Input

Since the magnitude of the control input is limited, the magnitude of the desired angular velocity and the desired angular acceleration shall be bounded as well. Hence we assume that

$$\max\{\|\Omega_d\|,\ \|\dot{\Omega}_d\|\} \leq B_d, \tag{35}$$

where $B_d \in \Re^+$ is a positive constant.

Proposition 4. Consider the attitude dynamic given by Eq. (1) and (2) with a desired relative attitude trajectory given by Eq. (8), the system is under the following control law: if $\|e_\Omega\| > B_W$, where $B_W \triangleq \sqrt{\frac{2k_R}{\lambda_M}[\psi - \Psi(R(0), R_d(0))]} \in \Re$,

$$u = -k_\Omega \mathfrak{sat}(e_\Omega) + JQ\dot{\Omega}_d + \widehat{Q\Omega}_d(JQ\Omega_d). \tag{36}$$

Otherwise,

$$u = -k_R e_R - k_\Omega \mathfrak{sat}(e_\Omega) + JQ\dot{\Omega}_d + \widehat{Q\Omega}_d(JQ\Omega_d). \tag{37}$$

The zero equilibrium of the tracking error, i.e., $(e_R,\, e_\Omega) = (0,\, 0)$ is exponentially stable.

Proof. The proof is devided to three part. In the first part, we manage to show that there is an upper bound of the control input. Secondly, we show boundedness of e_Ω by applying the first control input, namely, Eq. (36). Finally, the exponential stability is shown by using the second control input, Eq. (37).

1. Bounded Control Input

Identifying Eq. (35) as the upper bound of Ω_d and $\dot{\Omega}_d$, we have

$$\lambda_m B_d \leq JQ\dot{\Omega}_d \leq \lambda_M B_d,$$
$$\lambda_m B_d^2 \leq \widehat{Q\Omega}_d(JQ\Omega_d) \leq \lambda_M B_d^2,$$

where λ_m is the smallest eigenvalue of J. Note that $Q \in \mathsf{SO(3)}$ is a rotation matrix. Any vector multiplied by rotation matrices preserves its magnitude. Specifically, the angular velocity error vector e_Ω is bounded by $\mathfrak{sat}(\cdot)$ and Eq. (15) shows that the attitude error vector e_R itself is limited. Hence, both of the two control inputs are said to be bounded.

2. Ultimate Boundedness of e_Ω

We first define

$$\mathcal{U}_1(e_\Omega) = \frac{1}{2} e_\Omega^\mathsf{T} J e_\Omega,$$

which is positive definite with respect to e_Ω, that is, $\lambda_m \|e_\Omega\|^2 \leq \mathcal{U}_1(e_\Omega) \leq \lambda_M \|e_\Omega\|^2$. In particular, we can obtain time-derivative of $\mathcal{U}_1$ by using Eq. (19) and Eq. (36),

$$\dot{\mathcal{U}}_1 = e_\Omega^\mathsf{T} J \dot{e}_\Omega = e_\Omega^\mathsf{T}(-k_\Omega \mathfrak{sat}(e_\Omega) + \hat{\xi} e_\Omega) = \begin{cases} -k_\Omega \|e_\Omega\|^2, & \text{for } \|e_\Omega\| > 1 \\ -k_\Omega \|e_\Omega\|, & \text{for } \|e_\Omega\| \leq 1 \end{cases}$$

Notice that

$$\dot{\mathcal{U}}_1 \leq -W(e_\Omega),\ \forall \|e_\Omega\| \geq B_W > 0, \tag{38}$$

where

$$W(e_\Omega) = \begin{cases} k_\Omega, & \text{for } \|e_\Omega\| > 1 \\ k_\Omega \|e_\Omega\|^2, & \text{for } \|e_\Omega\| \leq 1 \end{cases}$$

Since $W(e_\Omega)$ is positive definite with respect to e_Ω, we can conclude that the solutions are uniformly ultimately bounded.[12]

3. Exponential Stability

Define

$$\mathcal{U}_2(R, R_d, e_\Omega) = \frac{1}{2} e_\Omega^\mathsf{T} J e_\Omega + k_R \Psi.$$

Using (17) and (37), the time-derivative of $\mathcal{U}_2$ yields to

$$\dot{\mathcal{U}}_2 = e_\Omega^\mathsf{T} J \dot{e}_\Omega + k_R \dot{\Psi} = e_\Omega^\mathsf{T}(-k_R e_R - k_\Omega \mathfrak{sat}(e_\Omega) + \hat{\xi} e_\Omega) + k_R e_\Omega^\mathsf{T} e_R = \begin{cases} -k_\Omega \|e_\Omega\|^2, & \text{for } \|e_\Omega\| > 1 \\ -k_\Omega \|e_\Omega\|, & \text{for } \|e_\Omega\| \leq 1 \end{cases}$$

which implies that $\mathcal{U}_2$ is a non-increasing function. To specify the initial condition of $\mathcal{U}_2$ with the estimate region of attraction

$$\|e_\Omega(0)\|^2 \leq \frac{2k_R}{\lambda_M}[\psi - \Psi(R(0), R_d(0))], \tag{39}$$

we have,

$$\begin{aligned} U_2(R(0), R_d(0), e_\Omega(0)) &\leq \frac{1}{2}\lambda_M \|e_\Omega(0)\|^2 + k_R \Psi(R(0), R_d(0)) \\ &\leq \frac{1}{2}\lambda_M \{\frac{2k_R}{\lambda_M}[\psi - \Psi(R(0), R_d(0))]\} + k_R \Psi(R(0), R_d(0)) = k_R \psi. \end{aligned} \tag{40}$$

Since $\mathcal{U}_2(t)$ is non-increasing, the value of $\mathcal{U}_2(t)$ must be less or equal than $\mathcal{U}(0)$ and it is known that $k_R\Psi \leq \mathcal{U}_2$, thus we can write

$$k_R\Psi(R(t), R_d(t)) \leq \mathcal{U}_2(R(t), R_d(t), e_\Omega(t)) \leq \mathcal{U}_2(R(0), R_d(0), e_\Omega(0)) \leq k_R\psi < k_R h_1, \tag{41}$$

which is consistent with (27).

The Lyapunov function is given as

$$\mathcal{V} = \frac{1}{2}e_\Omega^\mathsf{T} J e_\Omega + k_R\Psi + c e_R^\mathsf{T} J e_\Omega, \tag{42}$$

Using Eq. (14), we can obtain the upper bound and lower bound of $\mathcal{V}$.

$$z^\mathsf{T} M_1 z^\mathsf{T} \leq \mathcal{V} \leq z^\mathsf{T} M_2 z^\mathsf{T}, \tag{43}$$

where $z = \begin{bmatrix} \|e_R\| & \|e_\Omega\| \end{bmatrix}^\mathsf{T} \in \Re^2$, $M_1 = \frac{1}{2}\begin{bmatrix} 2b_1 & -c\lambda_M \\ -c\lambda_M & \lambda_m \end{bmatrix} \in \Re^{2\times 2}$ and $M_2 = \frac{\lambda_M}{2}\begin{bmatrix} \frac{2b_2}{\lambda_M} & c \\ c & 1 \end{bmatrix}$. As long as the constant c satisfying

$$c < \min\{\frac{\sqrt{2b_1\lambda_m}}{\lambda_M}, \sqrt{\frac{2b_2}{\lambda_M}}\},$$

the matrix M_1 M_2 are positive definite. This shows that V is positive definite.

The time-derivative of $\mathcal{V}$ is given as

$$\begin{aligned}\dot{\mathcal{V}} &= e_\Omega^\mathsf{T} J\dot{e}_\Omega + k_R\dot{\Psi} + c\dot{e}_R J e_\Omega^\mathsf{T} + c e_R^\mathsf{T} J\dot{e}_\Omega \\ &\leq (e_\Omega + c e_R)^\mathsf{T}[u + \xi \times e_\Omega - JQ\dot{\Omega}_d - \widehat{Q\Omega}_d(JQ\Omega_d)] + k_R e_\Omega^\mathsf{T} e_R + \frac{1}{\sqrt{2}}c\lambda_M \mathrm{tr}[G]\|e_\Omega\|^2,\end{aligned}$$

where Eq. (17) , (18) and (19) are applied. Then, substituting Eq. (37) with arrangement we obtain

$$\begin{aligned}\dot{\mathcal{V}} &\leq (e_\Omega + c e_R)^\mathsf{T}[\xi \times e_\Omega - k_R e_R - k_\Omega \mathfrak{sat}(e_\Omega)] + k_R e_\Omega^\mathsf{T} e_R + \frac{1}{\sqrt{2}}c\lambda_M \mathrm{tr}[G]\|e_\Omega\|^2 \\ &\leq -k_\Omega e_\Omega^\mathsf{T}\mathfrak{sat}(e_\Omega) + \frac{1}{\sqrt{2}}c\lambda_M \mathrm{tr}[G]\|e_\Omega\|^2 - ck_R\|e_R\|^2 - ck_\Omega e_R^\mathsf{T}\mathfrak{sat}(e_\Omega) + c\|e_R\|\|\xi\|\|e_\Omega\|.\end{aligned} \tag{44}$$

Recall Eq. (15) and (23), we have

$$\dot{\mathcal{V}} \leq -k_\Omega e_\Omega^\mathsf{T}\mathfrak{sat}(e_\Omega) + \frac{c\lambda_M}{2}(\sqrt{2}\mathrm{tr}[G] + \sqrt{12h_2 + 3h_3})\|e_\Omega\|^2 - ck_R\|e_R\|^2 - ck_\Omega e_R^\mathsf{T}\mathfrak{sat}(e_\Omega) + cB^*\|e_\Omega\|\|e_R\|.$$

If $\|e_\Omega\| \leq 1$,

$$\dot{\mathcal{V}} \leq -(k_\Omega - \frac{c\lambda_M}{2}(\sqrt{2}\mathrm{tr}[G] + \sqrt{12h_2 + 3h_3})\|e_\Omega\|^2 - ck_R\|e_R\|^2 + c(B^* + k_\Omega)\|e_\Omega\|\|e_R\| = -z^\mathsf{T} M_3 z, \tag{45}$$

where $M_3 = \frac{c}{2}\begin{bmatrix} 2k_R & -(B^* + k_\Omega) \\ -(B^* + k_\Omega) & \frac{2k_\Omega}{c} - (\sqrt{2}\mathrm{tr}[G] + \sqrt{12h_2 + 3h_3})\lambda_M \end{bmatrix} \in \Re^{2\times 2}$. If the constant c is chosen to satisfy the following condition,

$$c < \frac{k_R k_\Omega}{\frac{1}{2}(B^* + k_\Omega)^2 + k_R(\sqrt{2}\mathrm{tr}[G] + \sqrt{12h_2 + 3h_3})\lambda_M}, \tag{46}$$

the matrix M_3 is positive constant. Hence, we can conclude that $\dot{\mathcal{V}}$ is negative definite and the zero equilibrium is exponentially stable.

In conclusion, to achieve the exponential stability, the following two conditions must be satisfied

(a) $\|e_\Omega(0)\| \leq B_W$,

(b) $\|e_\Omega(t)\| \leq 1$,

where (a) is derived from the estimate region of attraction, Eq. (39), and (b) is from the intrinsic property of the saturation function, $\mathfrak{sat}(\cdot)$. Since our thrust model only allows a very low control input, the proportional gain k_R is much less then 1. Thus, we have $B_W < 1$ in this specific thrust model. Assuming $e_\Omega(0)$ is sufficiently large, we first apply Eq. (36) to the system as the control input such that $\|e_\Omega(t)\|$ will keep decreasing since it is uniformly ultimately bounded. Once $\|e_\Omega\|$ enters the region of attraction, the control input is switched to Eq. (37) such that both (a) and (b) are satisfied. Then, we can guarantee the exponential stability. □

D. PID Attitude Tracking with Bounded Control Input

The attitude error and the angular velocity error, e_R and e_Ω, in Proposition 3 and 4 stand for the proportional term and the derivative term, respectively. That is, the corresponding controllers are nonlinear PD controller. Here we introduce the integral term, $e_I \in \Re^3$, denoted by

$$e_I = \int_0^t ce_R + e_\Omega \, d\tau. \tag{47}$$

Proposition 5. Consider the same system in the Proposition 4, is under the following control law: if $\|e_\Omega\| > B_W$, where $B_W \triangleq \sqrt{\frac{2k_R}{\lambda_M}[\psi - \Psi(R(0), R_d(0))]} \in \Re$,

$$u = -k_\Omega \mathfrak{sat}(e_\Omega) + JQ\dot{\Omega}_d + \widehat{Q\Omega}_d(JQ\Omega_d). \tag{48}$$

Otherwise,

$$u = -k_I \mathfrak{sat}(e_I) - k_R e_R - k_\Omega \mathfrak{sat}(e_\Omega) + JQ\dot{\Omega}_d + \widehat{Q\Omega}_d(JQ\Omega_d), \tag{49}$$

where $k_I \in \Re^+$ is a positive constant. The zero equilibrium of the tracking error, i.e., (e_R, e_Ω, e_I) = (0, 0, 0) is stable.

Proof. Eq. (48) is same as Eq. (36). Since we are applying the same control strategy with the PD tracking case. The first and second part, input saturation and ultimate boundedness of $\|e_\Omega\|$, are proved in Proposition 4. To show the stability, we can start from the corresponding Lyapunov function.

$$\mathcal{V} = \frac{1}{2} e_\Omega^\mathsf{T} J e_\Omega + k_R \Psi + c e_R^\mathsf{T} J e_\Omega + k_I e_I^\mathsf{T} \mathfrak{sat}(e_I), \tag{50}$$

which is positive definite. The rate change of V is:

$$\dot{\mathcal{V}} = e_\Omega^\mathsf{T} J \dot{e}_\Omega + k_R \dot{\Psi} + c\dot{e}_R J e_\Omega^\mathsf{T} + c e_R^\mathsf{T} J \dot{e}_\Omega + \frac{d}{dt}(k_I e_I^\mathsf{T} \mathfrak{sat}(e_I)). \tag{51}$$

Knowing that

$$\begin{aligned} \frac{d}{dt}\big(e_I^\mathsf{T} \mathfrak{sat}(e_I)\big) &= \dot{e}_I^\mathsf{T} \mathfrak{sat}(e_I) + e_I^\mathsf{T} \big[\frac{d}{dt} \mathfrak{sat}(e_I)\big] \\ &= \frac{1}{\|e_I\|} e_I^\mathsf{T} \dot{e}_I + e_I^\mathsf{T} \big[\big(-\frac{1}{\|e_I\|^3} e_I^\mathsf{T} \dot{e}_I\big) e_I + \frac{1}{\|e_I\|} \dot{e}_I\big] = \frac{1}{\|e_I\|} e_I^\mathsf{T} \dot{e}_I = \mathfrak{sat}(e_I)^\mathsf{T} \dot{e}_I. \end{aligned} \tag{52}$$

With Eq. (17) , (18) and (19) in hands, we can rewrite $\dot{\mathcal{V}}$ in the form

$$\begin{aligned} \dot{\mathcal{V}} &= e_\Omega^\mathsf{T} J \dot{e}_\Omega + k_R \dot{\Psi} + c\dot{e}_R J e_\Omega^\mathsf{T} + c e_R^\mathsf{T} J \dot{e}_\Omega + k_I \mathfrak{sat}(e_I)^\mathsf{T} \dot{e}_I \\ &\le (e_\Omega + c e_R)^\mathsf{T} [u + \xi \times e_\Omega - JQ\dot{\Omega}_d - \widehat{Q\Omega}_d(JQ\Omega_d)] + k_R e_\Omega^\mathsf{T} e_R + \frac{1}{\sqrt{2}} c\lambda_M \mathrm{tr}[G] \|e_\Omega\|^2 + k_I \mathfrak{sat}(e_I)^\mathsf{T} \dot{e}_I. \end{aligned}$$

Then, substituting Eq. (47) and (49) with arrangement we obtain

$$\begin{aligned} \dot{\mathcal{V}} &\le (e_\Omega + c e_R)^\mathsf{T} [\xi \times e_\Omega - k_R e_R - k_I \mathfrak{sat}(e_I) - k_\Omega \mathfrak{sat}(e_\Omega)] + k_R e_\Omega^\mathsf{T} e_R \\ &\quad + \frac{1}{\sqrt{2}} c\lambda_M \mathrm{tr}[G] \|e_\Omega\|^2 + k_I \mathfrak{sat}(e_I)^\mathsf{T} (c e_R + e_\Omega) \\ &\le -k_\Omega e_\Omega^\mathsf{T} \mathfrak{sat}(e_\Omega) + \frac{1}{\sqrt{2}} c\lambda_M \mathrm{tr}[G] \|e_\Omega\|^2 - c k_R \|e_R\|^2 - c k_\Omega e_R^\mathsf{T} \mathfrak{sat}(e_\Omega) + c\|e_R\| \|\xi\| \|e_\Omega\|, \end{aligned}$$

which is same as Eq. (44). Hence, $\dot{\mathcal{V}}$ is negative semi-definite which implies the stability of the equlibrium. □

IV. Numerical Simulation

The trust model has been stated in Section B. The initial condition is chosen as follows:

$$R(0) = \exp(\frac{\pi}{2}\hat{e}_1), \quad \Omega(0) = [0.03, -0.04, 0.02] \text{ rad/sec},$$

where $e_1 = [1\ 0\ 0]^\mathsf{T}$. The matrix G is selected to be $G = \text{diag}[1.1,\ 1,\ 0.9]$. Consider the following cases:

A. Attitude Stabilization with Bounded Control Input

To detumble the CubeSta, $R_d = I$ and $\Omega_d = [0, 0, 0]$ where I is the 3 by 3 identity matrix. The controller gains are chosen as

$$k_R = 1 \times 10^{-7} \times \text{diag}[0.32,\ 0.16,\ 0.416], \quad k_\Omega = 1 \times 10^{-4} \times \text{diag}[0.56,\ 0.28,\ 0.728],$$

Notice that k_R and k_Ω are assigned to be scalars throughout this paper since we assumed the control inputs for each axis of the CubeSat are the same. Once we consider the geometry of the CubeSat, different control gains can be selected for different axes. Hence k_R and k_Ω can be generalized to positive definite diagonal matrices. The numerical result of detumbling is illustrated at Fig. 1.

B. PD Attitude Tracking with Bounded Control Input

The desired attitude is given in terms of 3-2-1 Euler angles as $R_d(t) = R_d(\alpha(t), \beta(t), \gamma(t))$ where $\alpha(t)$, $\beta(t)$, and $\gamma(t)$ are $0.0001\sin(0.2t)$, $0.0003\cos(0.1t)$ and 0, respectively. In addition, computing that $h_1 = 1.9$, $\Psi(R(0), R_d(0)) = 0.95$, $\lambda_M = 0.065$ and selecting $\psi = 1.8$. We therefore obtain

$$B_W = 0.007.$$

The corresponding result is shown at Fig. 2.

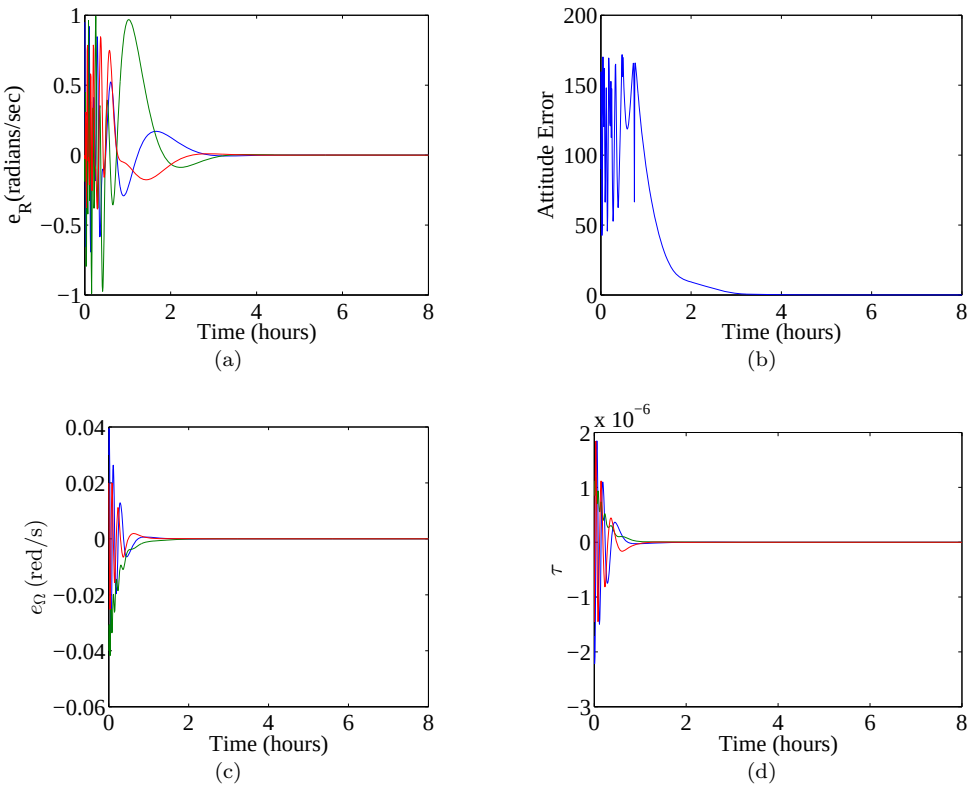

Figure 1. Attitude Stabilizing: (a)attitude error vector, (b)attitude error, (c)angular velocity error, (d)control input.

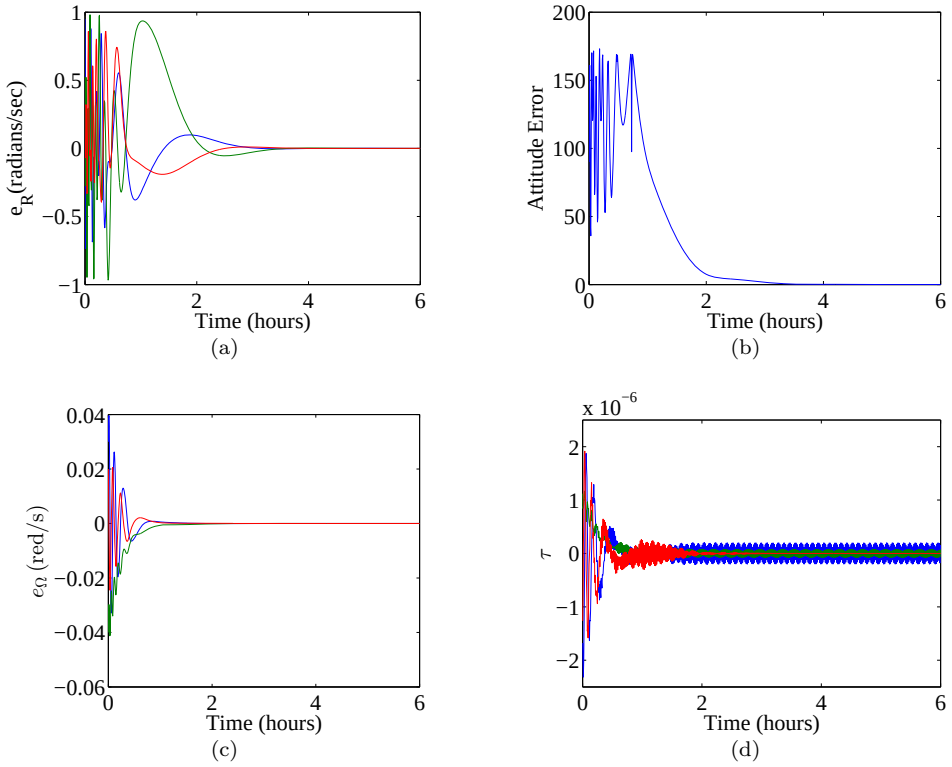

Figure 2. Attitude tracking: (a)attitude error vector, (b)attitude error, (c)angular velocity error, (d)control input.

C. PID Attitude Tracking with Bounded Control Input

In this model, the maximum torque is increased to $\tau_{max} = 2 \times 10^{-5}$Nm. The corresponding control gain are given as

$$k_R = 1 \times 10^{-5} \times \text{diag}[0.32,\ 0.16,\ 0.416], \quad k_\Omega = 1 \times 10^{-3} \times \text{diag}[0.56,\ 0.28,\ 0.728],$$

The desired attitude is given in terms of 3-2-1 Euler angles as $R_d(t) = R_d(\alpha(t), \beta(t), \gamma(t))$ where $\alpha(t) = 0$, $\beta(t) = 0.003\cos(0.8t)$, and $\gamma = 0.001\sin(0.5t)$. Moreover, the switched point is found to be

$$B_W = 0.0304.$$

Fig. 3 illustrates the result of applying first control input, which shows the ultimately boundedness of e_Ω. The switch point happens at $t = 0.0805$min where $\|e_\Omega\| = 0.0304 = B_W$. The angular velocity at the switch point, $\Omega = [0.0243, -0.01846, 0.001459]^\mathsf{T}$rad/s, and the corresponding attitude are set to be the initial conditions for the second part of the simulation. Fig. 4 shows the numerical distributions after switching to the second control input.

In spacecraft missions, control systems are subjected to disturbances and uncertainties, and PID controller is featured to eliminate the effect of fixed perturbation. Once the disturbances and uncertainties are considered, the equation of motion can be written as

$$\dot{\Omega} = J^{-1}(u - \Omega \times J\Omega) + \Delta, \tag{53}$$

where $\Delta \in \Re^3$ is the fixed perturbation which is specified to be $\Delta = [0.0001, 0.0002, -0.0001]^\mathsf{T}$ in this simulation model.

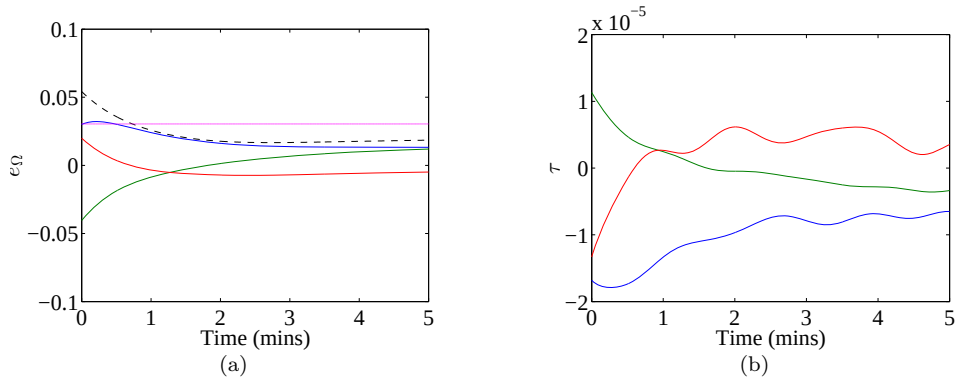

Figure 3. (a)Angular velocity error vector, the black dashed line and the magenta line represent $\|e_\Omega\|$ and B_W, respectively. The first control input successfully reduces the magnitude of e_Ω to the switch point in 1 minute. (b)Control input.

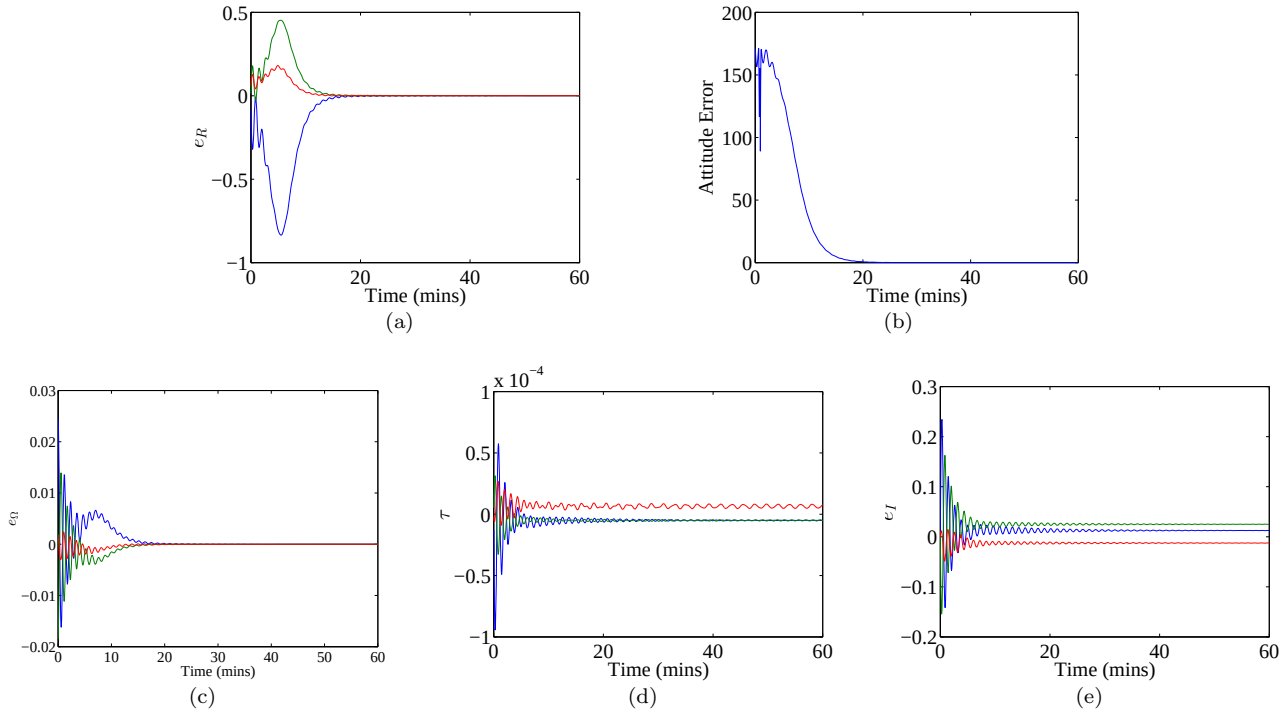

Figure 4. PID Attitude tracking: (a)attitude error vector, (b)attitude error, (c)angular velocity error, (d)control input, (e)integral error vector.

V. Conclusion

Based on the propulsion model of Micro-cathode arc thruster (μCAT), a continuous and bounded control law is presented to stabilize the CoubeSat and a discontinuous and bounded tracking control system is also developed. Since the propulsion of the μCATis quite small, it takes hours to stabilize the CubeSat and the magnitude of the tracking command is also restricted. Furthermore, a nonlinear PID controller is developed, and the feature of robustness to fixed perturbations is observed by numerical results.

References

[1]T. Zhuang, A. Shashurin, D. Chiu, G. Teel, and M. Keidar, "Micor-cathode arc thruster developement and characterization," in *Presented at the 32nd International Electric Propulsion Conference*, no. 266, 2011.

[2]T. Zhuang, A. Shashurin, S. Haque, and M. Keidar, "Performance characterization of the micro-cathode arc thruster and propulsion system for space applications," in *Joint Propulsion Conference and Exhibit*, vol. 46, no. AIAA-2010-7018, 2010.

[3]J. D. BoSkoviC, S.-M. Li, and R. K. Mehra, "Globally stable adaptive tracking control design for spacecraft under input saturation," in *IEEE Conference on Decision & Control*, 1999, pp. 1952–1957.

[4]J. Guerrero-Castellanos, H. Rifaï, N. Marchand, and G. Poulin, "Bounded attitude stabilization of rigid bodies without attitude estimation and velocity measurement," in *IEEE International Conference on Robotics and Biomimetics*, 2009, pp. 2203–2209.

[5]N. A. Chaturvedi and N. H. McClamroch, "Attitude stabilization of the inverted 3d pendulum on TSO(3) with control saturation," in *IEEE Conference on Decision and Control*, 2007, pp. 1910–1915.

[6]Q. Tang, Y. Wang, X. Chen, and Y. Lei, "Nonlinear attitude control of rigid body with bounded control input and velocity-free," in *IEEE International Conference on Robotics and Biomimetics*, 2009, pp. 2221–2226.

[7]B. Zhang and S. Song, "Robust attitude coordination control of formation flying spacecraft under control input saturation," *International Journal of Innovative Computing, Information and Control*, vol. 7, no. 7, pp. 4223–4235, 2011.

[8]J. Lv, D. Gao, and X. Zhang, "Attitude coordination control of spacecraft formation flying with bounded control inputs," in *IEEE Conference on Industrial Electronics and Applications (ICIEA)*, 2011, pp. 2096–2100.

[9]T. Lee, "Exponential stability of an attitude tracking control system on SO(3) for large-angle rotational maneuvers," *Systems and Control Letters*, vol. 61, no. 1, pp. 231–237, 2012.

[10]N. Chaturvedi, A. Sanyal, and N. McClamroch, "Rigid-body attitude control," *IEEE Control Systems Magazine*, vol. 31, no. 3, pp. 30–51, 2011.

[11]C. G. Mayhew, R. G. Sanfelice, and A. R. Teel, "On quaternion-based attitude control and the unwinding phenomenon," in *American Control Conference*, 2011, pp. 299–304.

[12]H. K. Khalil, *Nonlinear Systems*. Upper Saddle River, New Jersey: Prentice Hall, 2002.